

N/Z and N/A dependence of balance energy as a probe of symmetry energy in heavy-ion collisions

Aman D. Sood¹

*SUBATECH, Laboratoire de Physique Subatomique et des Technologies Associées,
Université de Nantes - IN2P3/CNRS - EMN 4 rue Alfred Kastler, F-44072 Nantes,
France.*

We study the N/Z and N/A dependence of balance energy (E_{bal}) for isotopic series of Ca having N/Z (N/A) varying from 1.0 to 2.0 (0.5 to 0.67). We show that the N/Z (N/A) dependence of E_{bal} is sensitive to symmetry energy and its density dependence at densities higher than saturation density and is insensitive towards the isospin dependence of nucleon-nucleon (nn) cross section and Coulomb repulsion. We also study the effect of momentum dependent interactions (MDI) on the N/Z (N/A) dependence of E_{bal} . We find that although MDI influences the E_{bal} drastically, the N/Z (N/A) dependence of E_{bal} remains unchanged on inclusion of MDI.

¹Email: amandsood@gmail.com

1 Introduction

With the availability of high-intensity radioactive beams at many facilities as well as a number of next generation beam facilities being constructed or being planned [1, 2], the studies on the role of isospin degree of freedom have recently attracted a lot of attention in both nuclear physics and astrophysics. The ultimate goal of such studies is to extract information on the isospin dependence of in-medium nuclear effective interactions as well as equation of state (EOS) of isospin asymmetric nuclear matter. The latter quantity especially the symmetry energy term is important not only to nuclear physics community as it sheds light on the structure of radioactive nuclei, reaction dynamics induced by rare isotopes but also to astrophysics community as it acts as a probe for understanding the evolution of massive stars and supernova explosion [3]. It is worth mentioning that the equation of state of symmetric nuclear matter has been constrained up to densities 5 times the normal nuclear matter density through the measurements of transverse flow as well as its disappearance along with other collective flows (like radial flow, elliptic flow) [4] and of subthreshold kaon production in relativistic nucleus-nucleus collisions [5].

Although the nuclear symmetry energy at normal nuclear matter density is known to be around 30 MeV [6], its values at other densities are poorly known. Heavy-ion collisions induced by radioactive beams provide unique opportunities to investigate the isospin-dependent properties of asymmetric nuclear matter, particularly the density dependence of symmetry energy [7]. Experimentally symmetry energy is not a directly measurable quantity and has to be extracted from observables related to symmetry energy. Over the last decade a large number of experimental observables have been proposed like neutron/proton ratio of emitted nucleons [8], the neutron-proton differential flow [9], the $t/{}^3\text{He}$ [10], π^-/π^+ [6, 11], Σ^-/Σ^+ [12], and K^0/K^+ [13] ratios and so on. A recent analysis of data has led to a symmetry energy term of the form $E_{sym} \simeq 31.6(\frac{\rho}{\rho_0})^\gamma$ MeV with $\gamma = 0.4-1.05$ for densities between $0.1\rho_0$ and $1.2\rho_0$ [14]. However, for all the above mentioned observables the Coulomb force of charged particles plays an important role. It competes strongly with symmetry energy. Recently Gautam and Sood [15] studied the relative contribution of Coulomb force and symmetry energy in isospin effects on the collective transverse flow as well as its disappearance for isobaric systems throughout the mass range and colliding geometry. They clearly demonstrated the dominance of Coulomb repulsion over the symmetry energy. The collective transverse in-plane flow disappears at

a particular energy called as balance energy [15, 16]. In recent communication, Gautam *et al.* [17] has studied the transverse momentum for a neutron rich system $^{60}\text{Ca}+^{60}\text{Ca}$ in the Fermi energy as well as at high energies. There they find that transverse momentum is sensitive to the symmetry energy as well as its density dependence in the Fermi energy region. Motivated by those results we here study the E_{bal} as a function of N/Z and N/A of the system for an isotopic series. We here choose the isotopes so that the Coulomb repulsion is same for all the systems, since as mentioned previously that Coulomb plays much dominant role as compared to symmetry energy in isospin effects. Here we will demonstrate that the N/Z (N/A) dependence of E_{bal} for the isotopes of same element is a sensitive probe for the symmetry energy as well as its density dependence. To check the sensitivity of N/Z (N/A) dependence of E_{bal} towards density dependence of symmetry energy, we have calculated the E_{bal} throughout the isotopic series for different forms of symmetry energy $F_1(u)$, $F_2(u)$, and $F_3(u)$, where $u = \frac{\rho}{\rho_0}$. The different forms are described later. The present study is carried out within the framework of Isospin-dependent Quantum Molecular Dynamics (IQMD)[18] Model. Section 2 describes the model in brief. Section 3 explains the results and discussion and section 4 summarizes the results.

2 The model

The IQMD model treats different charge states of nucleons, deltas and pions explicitly, as inherited from the Vlasov-Uehling-Uhlenbeck (VUU) model. The IQMD model has been used successfully for the analysis of a large number of observables from low to relativistic energies. One of its versions QMD model has been quite successful in explaining various phenomena such as multifragmentation [19], collective flow [20], and hot and dense nuclear matter [21] as well as particle production [22]. The isospin degree of freedom enters into the calculations via symmetry potential, cross sections and Coulomb interaction.

In this model, baryons are represented by Gaussian-shaped density distributions

$$f_i(\vec{r}, \vec{p}, t) = \frac{1}{\pi^2 \hbar^2} \exp(-[\vec{r} - \vec{r}_i(t)]^2 \frac{1}{2L}) \times \exp(-[\vec{p} - \vec{p}_i(t)]^2 \frac{2L}{\hbar^2}) \quad (1)$$

Nucleons are initialized in a sphere with radius $R = 1.12 A^{1/3}$ fm, in accordance with liquid-drop model. Each nucleon occupies a volume of h^3 , so that phase space is uniformly filled. The initial momenta are randomly chosen between 0 and Fermi momentum (\vec{p}_F). The nucleons of the target and projectile interact by two- and three-body Skyrme

forces, Yukawa potential, Coulomb interactions, and momentum-dependent interactions (MDI). In addition to the use of explicit charge states of all baryons and mesons, a symmetry potential between protons and neutrons corresponding to the Bethe-Weizsacker mass formula has been included. The hadrons propagate using Hamilton equations of motion:

$$\frac{d\vec{r}_i}{dt} = \frac{d\langle H \rangle}{d\vec{p}_i}; \quad \frac{d\vec{p}_i}{dt} = -\frac{d\langle H \rangle}{d\vec{r}_i} \quad (2)$$

with

$$\begin{aligned} \langle H \rangle &= \langle T \rangle + \langle V \rangle \\ &= \sum_i \frac{p_i^2}{2m_i} + \sum_i \sum_{j>i} \int f_i(\vec{r}, \vec{p}, t) V^{ij}(\vec{r}', \vec{r}) \\ &\quad \times f_j(\vec{r}', \vec{p}', t) d\vec{r} d\vec{r}' d\vec{p} d\vec{p}'. \end{aligned} \quad (3)$$

The baryon potential V^{ij} , in the above relation, reads as

$$\begin{aligned} V^{ij}(\vec{r}' - \vec{r}) &= V_{Skyrme}^{ij} + V_{Yukawa}^{ij} + V_{Coul}^{ij} + V_{mdi}^{ij} + V_{sym}^{ij} \\ &= [t_1 \delta(\vec{r}' - \vec{r}) + t_2 \delta(\vec{r}' - \vec{r}) \rho^{\gamma-1} (\frac{\vec{r}' + \vec{r}}{2})] \\ &\quad + t_3 \frac{\exp(|(\vec{r}' - \vec{r})|/\mu)}{(|(\vec{r}' - \vec{r})|/\mu)} + \frac{Z_i Z_j e^2}{|(\vec{r}' - \vec{r})|} \\ &\quad + t_4 \ln^2 [t_5 (\vec{p}' - \vec{p})^2 + 1] \delta(\vec{r}' - \vec{r}) \\ &\quad + t_6 \frac{1}{\varrho_0} T_{3i} T_{3j} \delta(\vec{r}' - \vec{r}). \end{aligned} \quad (4)$$

Here Z_i and Z_j denote the charges of i th and j th baryon, and T_{3i} and T_{3j} are their respective T_3 components (i.e., $1/2$ for protons and $-1/2$ for neutrons). The parameters μ and t_1, \dots, t_6 are adjusted to the real part of the nucleonic optical potential. For the density dependence of the nucleon optical potential, standard Skyrme-type parametrization is employed. We also use the isospin and energy-dependent cross section $\sigma = 0.8 \sigma_{nn}^{free}$. The details about the elastic and inelastic cross sections for proton-proton and proton-neutron collisions can be found in [18, 23]. The cross sections for neutron-neutron collisions are assumed to be equal to the proton-proton cross sections. Explicit Pauli blocking is also included; i.e. Pauli blocking of the neutrons and protons is treated separately. We assume that each nucleon occupies a sphere in coordinate and momentum space. This trick yields the same Pauli blocking ratio as an exact calculation of the overlap of the Gaussians will yield. We calculate the fractions P_1 and P_2 of final phase space for each of the two

scattering partners that are already occupied by other nucleons with the same isospin as that of scattered ones. The collision is blocked with the probability

$$P_{block} = 1 - [1 - \min(P_1, 1)][1 - \min(P_2, 1)], \quad (5)$$

and, correspondingly is allowed with the probability $1 - P_{block}$. For a nucleus in its ground state, we obtain an averaged blocking probability $\langle P_{block} \rangle = 0.96$. Whenever an attempted collision is blocked, the scattering partners maintain the original momenta prior to scattering. The different forms of symmetry energy are obtained by changing the density dependence of the potential part of the symmetry energy (last term in eq. (4)). The various forms are $F_1(u) \propto u$, $F_2(u) \propto u^{0.4}$, $F_3(u) \propto u^2$ (where $u = \frac{\rho}{\rho_0}$). F_4 represents calculations without symmetry potential.

3 Results and discussion

We have simulated several thousand events at incident energies around balance energy in small steps of 10 MeV/nucleon for each isotopic system of Ca+Ca having N/Z (N/A) varying from 1.0 to 2.0 (0.5-0.67). i.e. $\text{Ca}^{40}+\text{Ca}^{40}$, $\text{Ca}^{44}+\text{Ca}^{44}$, $\text{Ca}^{48}+\text{Ca}^{48}$, $\text{Ca}^{52}+\text{Ca}^{52}$, $\text{Ca}^{56}+\text{Ca}^{56}$, and $\text{Ca}^{60}+\text{Ca}^{60}$ for the semicentral colliding geometry range of 0.2 - 0.4. Such systematic studies performed at low incident energies using various fusion models have shown a linear enhancement in the fusion probabilities with neutron content [24]. We use soft equation of state with and without MDI, labeled respectively as Soft and SMD. The calculations with this choice of equation of state and cross section were in good agreement with the data throughout the colliding geometry [25]. The IQMD model has also been able to reproduce the other data (example, high energy proton spectra, gamma production) at incident energies relevant in this paper [26, 27]. The reactions are followed till the transverse flow saturates. The saturation time is around 100 fm/c for the systems in the present study. For the transverse flow, we use the quantity "directed transverse momentum $\langle p_x^{dir} \rangle$ " which is defined as [28, 29]

$$\langle p_x^{dir} \rangle = \frac{1}{A} \sum_{i=1}^A \text{sign}\{y(i)\} p_x(i), \quad (6)$$

where $y(i)$ is the rapidity and $p_x(i)$ is the momentum of i^{th} particle. The rapidity is defined as

$$Y(i) = \frac{1}{2} \ln \frac{\mathbf{E}(i) + \mathbf{p}_z(i)}{\mathbf{E}(i) - \mathbf{p}_z(i)}, \quad (7)$$

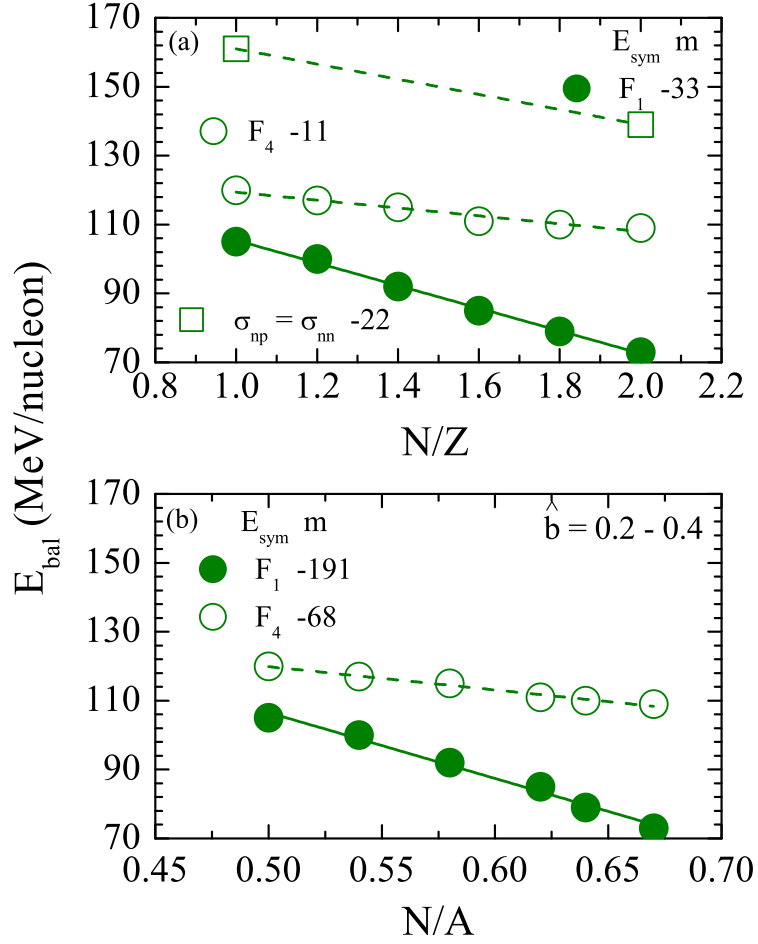


Figure 1: (Color online) E_{bal} as a function of N/Z (upper panel) and N/A (lower panel) of system for $E_{sym} \propto F_1(u)$ and F_4 . Lines are linear fit proportional to m . Various symbols are explained in the text.

where $\mathbf{E}(i)$ and $\mathbf{p}_z(i)$ are, respectively, the energy and longitudinal momentum of i^{th} particle. In this definition, all the rapidity bins are taken into account. A straight line interpolation is used to calculate the E_{bal} . It is worth mentioning that the E_{bal} has the same value for all fragments types [31–34].

In fig. 1(a) we display the E_{bal} as a function of N/Z of the system. Solid green circles represent the calculated E_{bal} . Lines are the linear fit to E_{bal} . We see that E_{bal} follows a linear behavior $\propto m \cdot N/Z$. As the N/Z of the system increases, the mass of the system increases due to addition of neutron content. In addition, the effect of symmetry energy also increases with increase in N/Z . To check the relative contribution of increase

in mass with N/Z and symmetry energy towards the N/Z dependence of E_{bal} , we make the strength of symmetry energy zero and calculate E_{bal} . The results are displayed by open circles in fig. 1(a). E_{bal} again follows a linear behavior $\propto m \cdot N/Z$. However, E_{bal} decreases very slightly with increase in N/Z , whereas when we include the symmetry energy also in our calculations then the $|m|$ increases by 3 times which shows that N/Z dependence of E_{bal} is highly sensitive to the symmetry energy. The slight decrease in the E_{bal} with N/Z (for calculations without symmetry energy) is due to increase in number of nucleon-nucleon collisions. To further explore this point, we switch off the symmetry energy and also make the cross section isospin independent (i.e. $\sigma_{np} = \sigma_{nn}$ and calculate E_{bal} for two extreme N/Z . The results are displayed in fig. 1(a) by open squares. Again E_{bal} follows a linear behavior. We see that the E_{bal} for both $^{40}\text{Ca} + ^{40}\text{Ca}$ and $^{60}\text{Ca} + ^{60}\text{Ca}$ increases as expected. However, the increase in E_{bal} for system with $N/Z = 1$ is more as compared to the system with $N/Z = 2$. This is because with increase in N/Z the neutron number increases due to which neutron-neutron and neutron-proton collisions pairs increase. However, the increase in number of neutron-neutron collision pairs is much larger as compared to neutron-proton collision pairs. Therefore, the possibility of neutron-proton collision is much less in system with $N/Z = 2$. That is why the effect of isospin dependence of cross section decreases with increase in N/Z .

In fig. 1(b), we display the E_{bal} as a function of N/A of the system. Symbols have same meaning as in fig. 1(a). Again E_{bal} follows a linear behaviour with $m = -191$ and -68 , respectively, for $F_1(u)$ and F_4 . However, the percentage difference $\Delta E_{bal} \%$ (where $\Delta E_{bal} \% = \frac{E_{bal}^{F_1(u)} - E_{bal}^{F_4}}{E_{bal}^{F_1(u)}}$) is same (about 65%) in both the figs. 1(a) and 1(b) which shows that the effect of symmetry energy is same whether we discuss in terms of N/Z or N/A .

As stated in literature, the isospin dependence of collective flow and its disappearance has been explained as the competition among various reaction mechanisms, such as, nn collisions, symmetry energy, surface property of the colliding nuclei and Coulomb force [30]. Here we aim to show that the N/Z and N/A dependence of E_{bal} is sensitive to the symmetry energy only. Since we are taking the isotopic series, the effect of Coulomb will be same for all the reactions. We have also checked that the N/Z dependence of E_{bal} is insensitive to the EOS of symmetric nuclear matter. Moreover, as mentioned previously, the equation of state of symmetric nuclear matter has been constrained up to densities five times the normal matter density. In the present case as the N/Z of the system increases, the number of neutrons also increases. Since we are using isospin-dependent

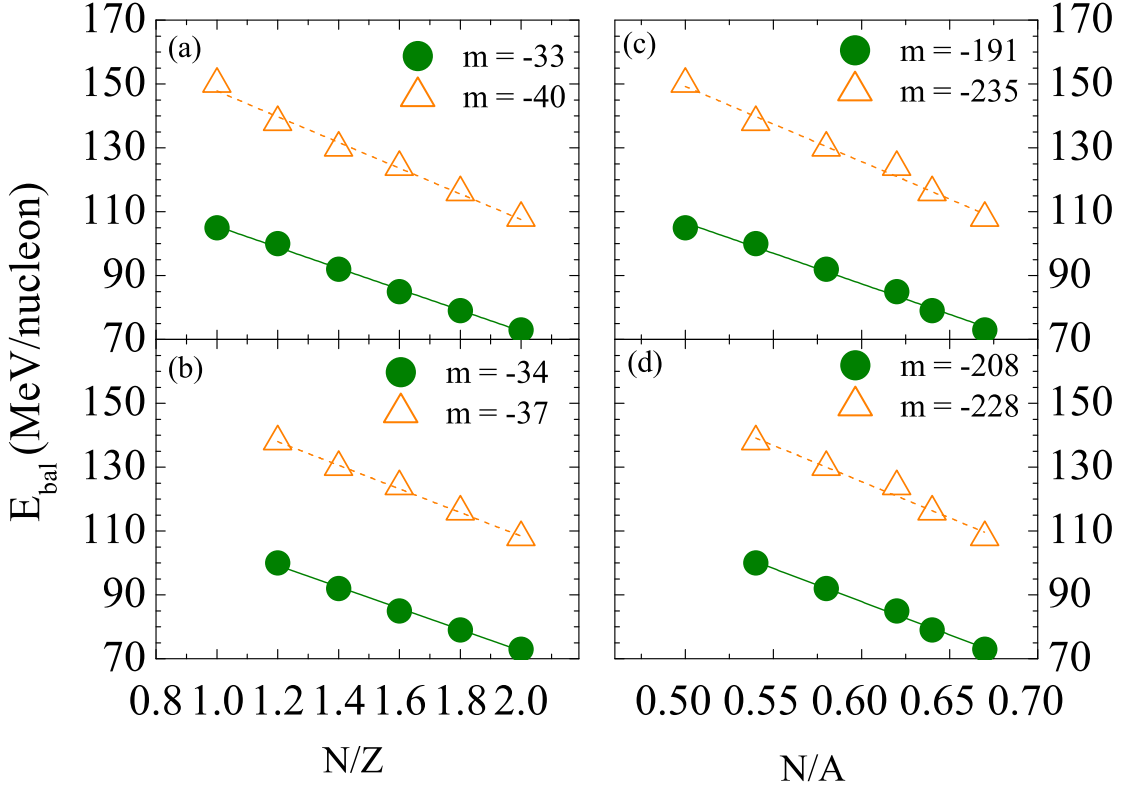


Figure 2: (Color online) E_{bal} as a function of N/Z (left panels) and N/A (right panels) of system for isospin independent cross section for (a) and (c) $N/Z = 1.0$ to 2.0 (b) and (d) $N/Z = 1.2$ to 2.0 . Lines are linear fit proportional to m . Various symbols are explained in the text.

nn cross section, so to check the sensitivity of N/Z and N/A dependence of E_{bal} to the isospin dependence of cross section, we calculate the E_{bal} throughout the isotopic series by making the cross section isospin independent (fig. 2(a) open orange triangles, left panels). Again E_{bal} follows a linear behavior with $m = -40$. We find that although E_{bal} for individual system is very sensitive to the isospin dependence of cross section. However, N/Z dependence of E_{bal} (for isotopic series) is much less sensitive to the isospin dependence of cross section.

In fig. 2(b) (left panels), we show E_{bal} as a function of N/Z of the system for the N/Z range from 1.2 to 2.0 . We find that the sensitivity of N/Z dependence of E_{bal} towards the isospin dependence of cross section decreases further. Now m is -34 (-37) for calculations

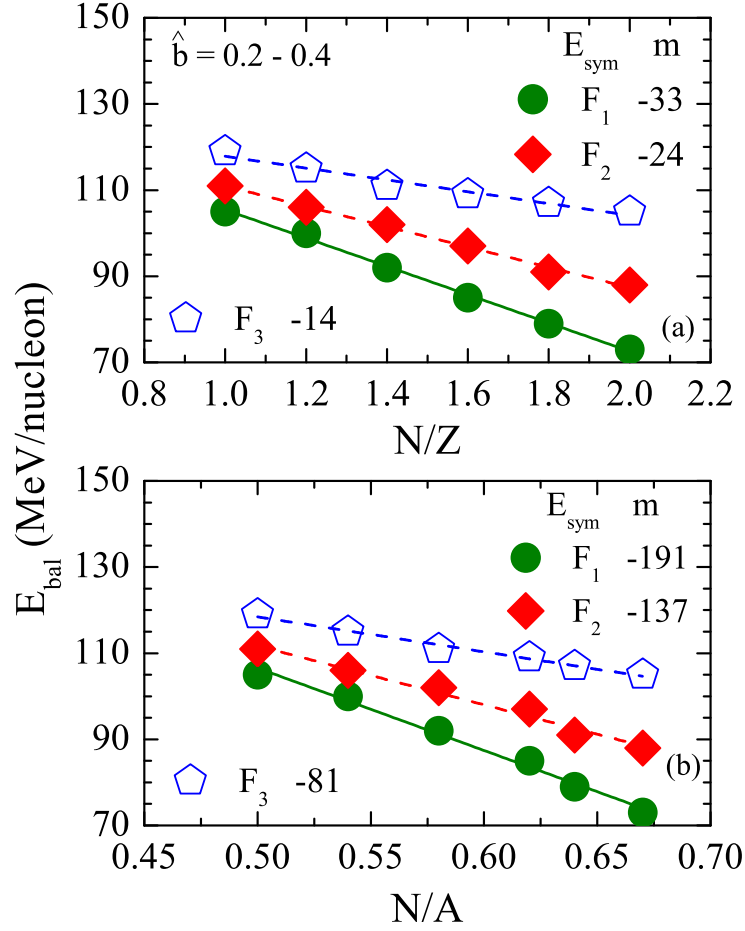


Figure 3: (Color online) E_{bal} as a function of N/Z (upper panel) and N/A (lower panel) of system for $E_{sym} \propto F_2(u)$ and $F_3(u)$. Lines are linear fit proportional to m . Various symbols are explained in the text.

with (without) isospin dependence of cross section. Thus the N/Z dependence of E_{bal} for neutron-rich isotopes is sensitive only to symmetry energy. In figs. 2(c) and 2(d) (right panels) we display similar plots as in the corresponding left panels but now we plot E_{bal} as a function of N/A of the system. Again the percentage difference between the two curves in both upper panels is same (about 18 %) and same in lower panels as well (about 8 %).

In fig. 3 (a) (3b) we display the N/Z (N/A) dependence of E_{bal} for different forms of symmetry energy; $F_1(u)$ (solid circles), $F_2(u)$ (diamonds), and $F_3(u)$ (pentagons). For all the cases E_{bal} follows a linear behavior. Clearly, N/Z (N/A) dependence of E_{bal} is sensitive to the density dependence of symmetry energy as well. For a fixed N/Z (N/A)

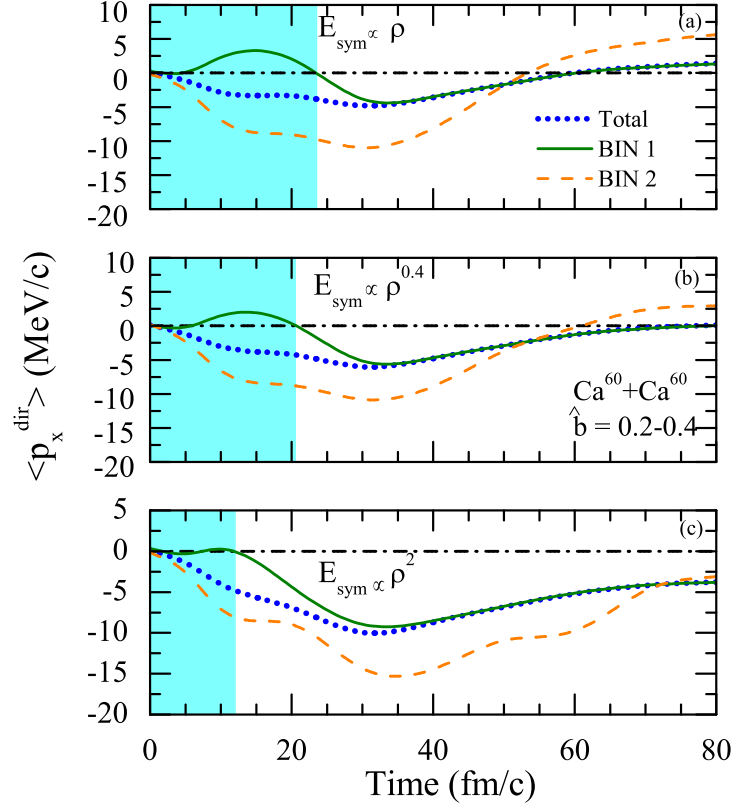


Figure 4: (Color online) The time evolution of $\langle p_x^{dir} \rangle$ for different forms of symmetry energy for different bins at $b/b_{max}=0.2-0.4$. Lines are explained in the text.

stiff symmetry energy $F_1(u)$ shows less E_{bal} as compared to soft $F_2(u)$ whereas super stiff symmetry energy $F_3(u)$ shows more E_{bal} as compared to $F_2(u)$.

To explain the above mentioned feature, we calculate for $^{60}\text{Ca} + ^{60}\text{Ca}$ the transverse flow of particles having $\rho/\rho_0 \leq 1$ (denoted as BIN 1) and particles with $\rho/\rho_0 > 1$ (denoted as BIN 2), separately at all time steps for symmetry energy $F_1(u)$, $F_2(u)$, and $F_3(u)$. The incident energy is taken to be 100 MeV/nucleon. The results are displayed in fig. 4. Solid (dashed) lines represent the p_x^{dir} of particles lying in BIN 1 (BIN 2). Dotted line represent the total $\langle p_x^{dir} \rangle$. We see that the total $\langle p_x^{dir} \rangle$ is maximum for stiff symmetry energy and minimum for super stiff symmetry energy. During the initial stages of the reaction, $\langle p_x^{dir} \rangle$ due to particles lying in BIN 1 remains positive for $F_1(u)$ and $F_2(u)$ because in the spectator region, repulsive symmetry energy will accelerate the particles away from the overlap zone. The effect is more pronounced for $F_1(u)$ as compared to $F_2(u)$. Moreover,

for $F_1(u)$ and $F_2(u)$, this interval is about 5-25 fm/c and 5-20 fm/c, respectively. This is because although for $F_2(u)$, the effective strength of symmetry energy will be more for low density particles as compared to $F_1(u)$, however, in the central dense zone the effective strength of $F_2(u)$ will be less i.e. in the central dense zone, $F_2(u)$ will be less repulsive, therefore for $F_2(u)$, there will be more attractive force on the particles lying in the spectator region towards the central dense zone as compared to that in case of $F_1(u)$. That is why during the initial stages the peak value of $\langle p_x^{dir} \rangle$ as well as the duration for which it remains positive is less for $F_2(u)$ as compared to $F_1(u)$ (compare shaded area in fig. 4(a) and 4(b)). This decides the value of $\langle p_x^{dir} \rangle$ at saturation, which is more for $F_1(u)$ as compared to $F_2(u)$. In case of $F_3(u)$ (fig. 4(c)) for particles lying in BIN 1, i.e. $(\rho/\rho_0 \leq 1)$, the strength of symmetry energy will be much smaller which is not sufficient to push the particles away from the overlap zone. Therefore, the $\langle p_x^{dir} \rangle$ of BIN 1 particles remains zero during the initial stages. This leads to least value of final state $\langle p_x^{dir} \rangle$ for super stiff symmetry energy as compared to stiff and soft symmetry energy. The $\langle p_x^{dir} \rangle$ due to particles in BIN 2 (dashed line) decreases in a very similar manner for all the different symmetry energies between 0-10 fm/c. Between 10-25 fm/c, $\langle p_x^{dir} \rangle$ for $F_3(u)$ decreases more sharply as compared to in case of $F_1(u)$ and $F_2(u)$. This is because in this time interval the particles from BIN 1 enters into BIN 2 and $\langle p_x^{dir} \rangle$ of particles entering BIN 2 from BIN 1 in case of $F_1(u)$ and $F_2(u)$ will be less negative due to stronger repulsive symmetry energy as compared to in case of $F_3(u)$ (see Ref. [17] also). During the expansion phase, i.e. after 30 fm/c the total $\langle p_x^{dir} \rangle$ and $\langle p_x^{dir} \rangle$ of BIN 1 particles overlap as expected. Therefore, the effect of symmetry energy on the low density particles during the initial stages decide the fate of the final $\langle p_x^{dir} \rangle$ and hence E_{bal} .

Since one cannot use radioactive isotopes as targets, therefore, as a next step we fix the target as a stable isotope ^{40}Ca and vary the projectile from ^{40}Ca to ^{60}Ca and calculate E_{bal} . In this case the N/Z (N/A) of the reaction varies between 1 to 1.5 (0.5 to 0.6) and the asymmetry $\delta = \frac{A_1 - A_2}{A_1 + A_2}$ of the reaction varies from 0 to 0.2. The results are displayed by solid green stars in figs. 5(a) and (b) (upper panels). The solid green circles represent the calculations for symmetric reactions with N/Z (N/A) varying from 1 to 2 (0.5 to 0.67), i.e. $^{40}\text{Ca} + ^{40}\text{Ca}$ to $^{60}\text{Ca} + ^{60}\text{Ca}$. Lines represent the linear fit $\propto m$. We see that N/Z (N/A) dependence of E_{bal} is same for both the cases. We also find that when we use stable target ^{40}Ca and radioactive target ^{60}Ca , the N/Z (N/A) decreases from 2 (0.67)

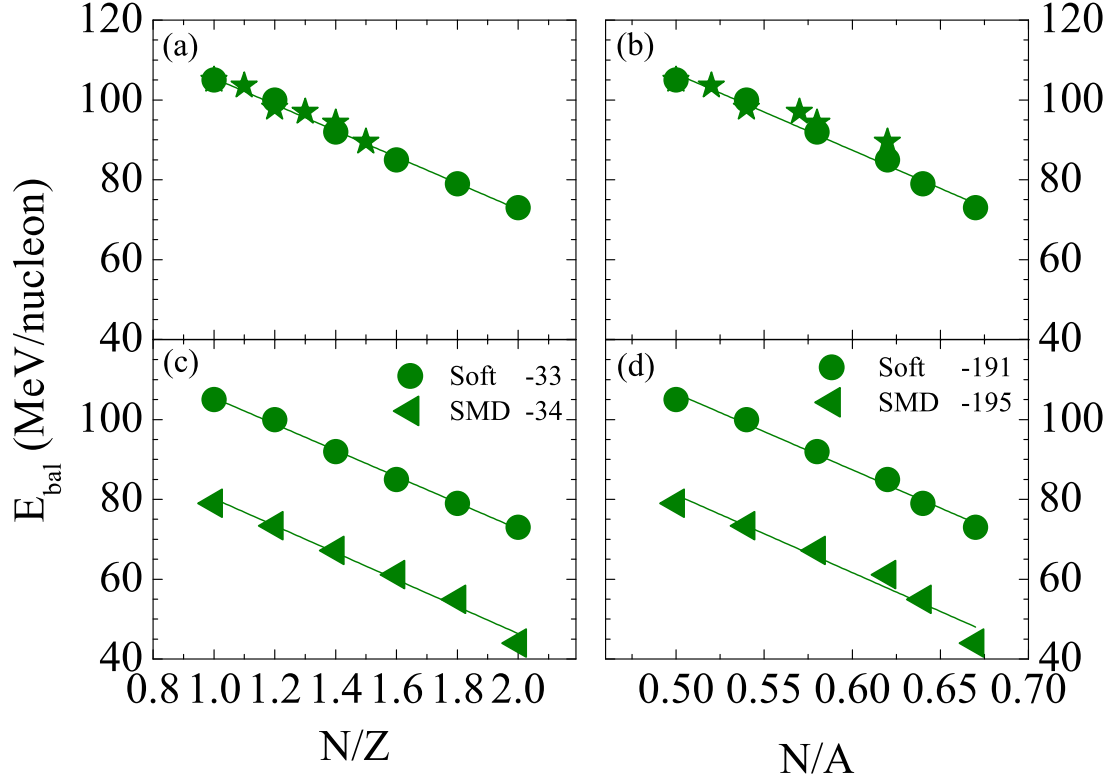


Figure 5: (a) and (b) (upper panels) E_{bal} as a function of N/Z (left panel) and N/A (right panel) of system for $E_{sym} \propto F_1(u)$ with ^{40}Ca as target (stars). (c) and (d) (lower panels) E_{bal} as a function of N/Z (left panel) and N/A (right panel) of system for $E_{sym} \propto F_1(u)$ with SMD EOS (left triangles). Circles represent the values of E_{bal} as in fig. 1. Lines are linear fit proportional to m .

in case of $^{60}\text{Ca}+^{60}\text{Ca}$ to 1.5 for $^{60}\text{Ca}+^{40}\text{Ca}$, so the E_{bal} also decreases. Now the E_{bal} for $^{60}\text{Ca}+^{40}\text{Ca}$ has same value as in case of symmetric reactions with N/Z (N/A) = 1.5 (0.6) i.e. the value of E_{bal} is decided by the N/Z (N/A) of the system and is independent of the asymmetry of the reaction in agreement with [35].

It has also been reported in literature that the MDI affects drastically the collective flow as well as its disappearance [36]. To check the influence of MDI on the N/Z (N/A) dependence of E_{bal} we calculate the E_{bal} for the whole N/Z (N/A) range from 1 to 2 (0.5 to 0.67) for the symmetric reactions with SMD equation of state and symmetry potential $F_1(u)$. The results are shown in figs. 5(c) and (d) (lower panels) by solid left triangles. We find that although the MDI changes drastically the absolute value of E_{bal} (by about

30%), however the N/Z (N/A) dependence of E_{bal} remains unchanged on inclusion of MDI. Therefore, the dependence of E_{bal} as a function of N/Z (N/A) on the symmetry energies of other different forms ($F_2(u)$ and $F_3(u)$) is also expected to be preserved on inclusion of MDI.

4 Summary

We have shown that the N/Z (N/A) dependence of E_{bal} for the isotopic series of Ca+Ca is a sensitive probe to the symmetry energy as well as its density dependence at densities higher than saturation density and is insensitive to other isospin effects like Coulomb repulsion, and isospin dependence of nucleon-nucleon cross section. We have also studied the effect of MDI on the N/Z (N/A) dependence of E_{bal} . We find that although MDI influences the E_{bal} drastically, the N/Z (N/A) dependence of E_{bal} remains unchanged on inclusion of MDI.

This work has been supported by a grant from Indo-French Centre For The Promotion Of Advanced Research (IFCPAR) under project no. 4104-1.

References

- [1] W. Zhan *et al.*, Int. J. Mod. Phys. E **15**, 1941 (2006); See, e.g., http://www.gsi.de/fair/index_e.html; See, e.g., <http://ganiinfo.in2p3.fr.research/developments/spiral2>.
- [2] Y. Yano, Nucl. Inst. Methods B **261**, 1009 (2007).
- [3] G. F. Marranghello *et al.*, Phys. Rev. C **81**, 024307 (2010); S. Kubis, Phys. Rev. C **76**, 025801 (2007).
- [4] P. Danielewicz *et al.*, Science, **298**, 1592 (2002).
- [5] C. Fuchs, Prog. Part. Nucl. Phys., **56**, 1 (2006).
- [6] B. A. Li, Phys. Rev. Lett. **88**, 192701 (2002); L. Chen *et al.*, Phys. Rev. C **68**, 017601 (2003).

- [7] B. A. Li *et al.*, Int. J. Mod. Phys. E **7**,147 (1998); V. Baran *et al.*, Phys. Rep. **411**, 335 (2005); B. A. Li, Phys. Rep. **464**, 113 (2008); B. A. Li and A. W. Steiner, Phys. Lett. B **642**, 436 (2006).
- [8] B. A. Li *et al.*, Phys. Rev. Lett. **78**, 1644 (1997).
- [9] B. A. Li, Phys. Rev. Lett. **85**, 421 (2000).
- [10] L. W. Chen *et al.*, Phys. Rev. C **68**, 017601 (2003); Nucl. Phys. A **729**, 809 (2003).
- [11] T. Gaitanos *et al.*, Nucl. Phys. A **732**, 24 (2004); Q. Li *et al.*, Phys. Rev. C **72**, 034613 (2005); J. Phys. G **32**, 151 (2006).
- [12] Q. Li *et al.*, Phys. Rev. C **71**, 054907 (2005).
- [13] G. Ferini *et al.*, Phys. Rev. Lett. **97**, 202301 (2006).
- [14] D. V. Shetty and S. J. Yennello, Pramana J. Phys. **75**, 259 (2010); M. B. Tsang, Y. Zhang, P. Danielewicz, M. Famiano, Z. Li, W. G. Lynch, and A. W. Steiner, Phys. Rev. Lett. **102**, 122701 (2009).
- [15] S. Gautam and A. D. Sood, Phys. Rev. C **82**, 014604 (2010); S. Gautam, A. D. Sood, R. K. Puri, and J. Aichelin, Phys. Rev. C **83**, 014603 (2011) .
- [16] D. Krofcheck *et al.*, Phys. Rev. Lett. **63**, 2028 (1989); A. Bonasera and L. P. Csernai, Phys. Rev. Lett. **59**, 630 (1987).
- [17] S. Gautam, A. D. Sood, R. K. Puri, and J. Aichelin, Phys. Rev. C **83**, 034606 (2011).
- [18] C. Hartnack *et al.*, Eur. Phys. J. A **1**, 151 (1998); C. Hartnack and J. Aichelin, Phys. Rev. C **49**, 2801 (1994); S. Kumar *et al.*, Phys. Rev. C **81**, 014601 (2010); *ibid.* **81**, 014611 (2010).
- [19] S. Kumar *et al.*, Phys. Rev. C **78**, 064602 (2008); Y. K. Vermani *et al.*, Phys. Rev. C **79**, 064613 (2009); *ibid.* Eur. Phys. Lett. **85**, 062001 (2009); *ibid.* J. Phys. G: Nucl. Part. Phys. **37**, 015105 (2010); *ibid.* **36**, 0105103 (2009).

- [20] A. D. Sood *et al.*, Phys. Rev. C **70**, 034611 (2004); *ibid.* **73**, 067602 (2006); *ibid.* **79**, 064618 (2009); *ibid.* Eur. Phys. J. A **30**, 571 (2006); S. Kumar *et al.*, Phys. Rev. C **58**, 3494 (1998).
- [21] E. Lehmann *et al.*, Phys. Rev. C **51**, 2113 (1995); *ibid.* Prog. Part. Phys. **30**, 219 (1993); Y. K. Vermani *et al.*, Nucl. Phys. A **847**, 243 (2010); C. Fuchs *et al.*, J. Phys. G: Nucl. Part. Phys. **22**, 131 (1996); G. Batko *et al.*, *ibid.* **20**, 461 (1994); R. K. Puri *et al.*, Nucl. Phys. A **575**, 733 (1994); D. T. Khoa *et al.*, Nucl. Phys. A **548**, 102 (1992); J. Singh *et al.*, Phys. Rev. C **67**, 044617 (2000).
- [22] S.W. Huang *et al.*, Phys Letts. B **41**, 298 (1993); *ibid.* Prog. Nucl. Part Phys. **30**, 105 (1993).
- [23] J. Cugnon, T. Mizutani, and J. Vandermeulen, Nucl. Phys. **A352** 505, 1981.
- [24] R. K. Puri *et al.*, Eur. Phys. J A **23**, 429 (2005); *ibid.* **A3**, 277 (1998); *ibid.* J Phys G: **18**, 903(1992); *ibid.*, **18** , 1533 (1992); *ibid.* Phys Rev C **43**, 315 (1991); *ibid.* , C45, 1837 (1992); R. Arora *et al.*, Eur. Phys. J A **8**, 103 (2008); I. Dutt *et al.*, Phys. Rev. C **81**, 064608 (2010); *ibid.* **81**, 064609 (2010); *ibid.* **81**, 047601 (2010); *ibid.* **81**, 044615 (2010).
- [25] S. Gautam, R. Chugh, A. D. Sood, R. K. Puri, C. Hartnack, and J. Aichelin, J. Phys.G: Nucl. Part. Phys. **37**, 085102 (2010).
- [26] M. Germain, C. Hartnack, J. L. Laville, J. Aichelin, M. Belkacem, and E. Suraud, Phys. Lett. **B437**, 19 (1998).
- [27] D. T. Khoa *et al.*, Nucl. Phys. **A529**, 363 (1991); G. Q. Li, Y. Lotfy, S. W. Huang, and A. Faessler, J. Phys. G:Nucl. Part. Phys. **18**, 291 (1992); S. W. Huang *et al.*, Progress in particle and nuclear physics **30**, 105 (1993).
- [28] A. D. Sood and R. K. Puri, Phys. Lett. **B594**, 260 (2004); *ibid.*, Phys. Rev. C **69**, 054612 (2004); R. Chugh *et al.*, Phys Rev C **82**, 014603(2010).
- [29] S. Kumar *et al.*, Phys Rev C **58**, 1618 (1998).
- [30] B. A. Li *et al.*, Phys. Rev. Lett. **76**, 4492 (1996); C. Liewen *et al.*, Phys. Rev. C **58**, 2283 (1998).

- [31] R. Pak R *et al.*, Phys. Rev. Lett **78**, 1022 (1997); *ibid.* **78**, 1026 (1997).
- [32] G. D. Westfall *et al.*, Phys. Rev. Lett. **71**, 1986 (1993).
- [33] G. D. Westfall, Nucl. Phys. **A630**, 27c (1998).
- [34] D. Cussol *et al.*, Phys. Rev. C **65**, 044604 (2002).
- [35] S. Goyal and R. K. Puri, Nucl. Phys. A **853**, 164 (2011); S. Goyal and R. K. Puri, Phys. Rev. C **30**, 571 (2011); J. Singh, S. Kumar and R. K. Puri, Phys. Rev. C **62**, 044617 (2000); *ibid.* **C63**, 054603 (2001); S. Goyal, S. Gautam, A. D. Sood, and R. K. Puri, Proceedings of International Symposium on Nuclear Physics, **54**, 450 (2009).
- [36] A. D. Sood and R. K. Puri, Eur. Phys. J. A **30**, 571 (2006); J. Aichelin, A. Rosenhauer, G. Peilert, H. Stoecker, and W. Greiner, Phys. Rev. Lett. **58**, 1926 (1987).